Analyst

Accepted Manuscript

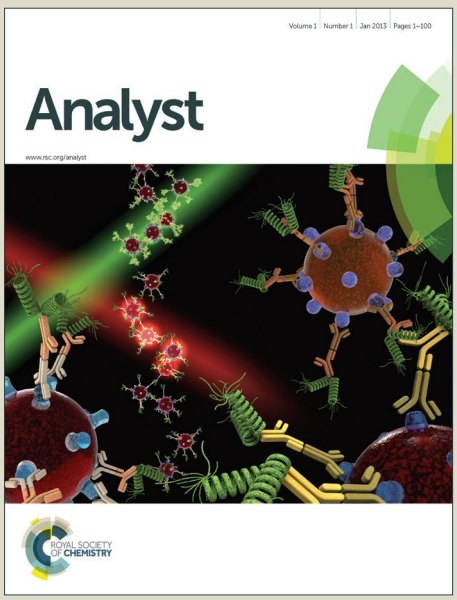

ROYAL SOCIETY OF CHEMISTRY

www.rsc.org/analyst

Cite this: DOI: 10.1039/c0xx00000x

www.rsc.org/xxxxxx ARTICLE TYPE

Sensitive and selective sensor for biothiols based on turn-on fluorescence of the Fe-MIL-88 metal-organic frameworks–hydrogen peroxide system

Zheng Juan Sun, Jun Ze Jiang, Yuan Fang Li*

Received (in XXX, XXX) Xth XXXXXXXXX 200X, Accepted Xth XXXXXXXXX 200X
DOI: 10.1039/b000000x

Herein, we present a novel strategy based on a "turn-on" fluorescence system made up of metal-organic frameworks Fe-MIL-88 and H_2O_2 for detecting biothiols in human serum. The nonfluorescent Fe-MIL-88 gives weak fluorescence in the presence of H_2O_2. Interestingly, it was found that the biothiols such as glutathione (GSH), cysteine (Cys) or homocysteine (Hcy) could induce fluorescence turn-on of the Fe-MIL-88/H_2O_2 system. Under optimal conditions, the relative fluorescence intensity exhibited good linear relationships in the range from 50 nM-10μM for GSH (r=0.994), 50 nM-10μM for Cys (r=0.990), and 50 nM-10μM (r=0.992) for Hcy, the detection limits of GSH, Cys and Hcy were 30 nM, 40 nM, and 40 nM respectively. Mechanism investigation reveals that biothiols could associate with Fe-MIL-88 via hydrogen bonding and electrostatic interaction followed by redox reaction between biothiols and Fe^{3+} consists in the Fe-MIL-88, Fe^{3+} was thus reduced to Fe^{2+}, then Fe^{2+} could efficiently catalyze the decomposition of H_2O_2 to yield •OH radicals through the Fenton reaction. Besides, biothiols was able to reduce H_2O_2 to produce •OH radicals directly. Thus the Fe-MIL-88 as well as biothiols could cooperatively contribute to the activation of H_2O_2 to generate more amounts of •OH radicals, which in turn oxidize the free ligand terephthalic acid (BDC) outside or within the Fe-MIL-88 structure to strongly fluorescent hydroxylated terephthalic acid (OHBDC), thereby turning on the fluorescence.

1 Introduction

Metal–organic frameworks (MOFs) are a fascinating class of crystalline materials originated through the self-assembly of organic linkers coordinated by metal ions or metal clusters.[1, 2] Due to the distinct properties of MOFs, such as high surface area, permanent porosity, well-defined structure and open metal sites, they have been widely utilized in chromatographic separation,[3-8] analytes enrichment,[9-12] catalysis,[13-15] chemical sensing,[16-20] gas storage and separation.[21, 22] As one of the important member in metal-organic frameworks family, the MIL-88(Fe) is extremely attractive due to their high catalytic activity. For example, MIL-88(Fe) which consists of Fe_3-μ_3-oxo clusters has been proven to possess photocatalytic activity under visible light illumination.[23] Moreover, due to the existence of the Fe-O clusters in its structure, MIL-88(Fe) can selectively photocatalytically reduce CO_2 to produce $HCOO^-$ under visible light.[24] Based on the same mechanism, it can also be used as photocatalyst for the reduction of Cr (VI).[25] Their high catalytic activity coupled with the nontoxic nature make them ideal candidates for new valuable nanomaterials for biological assay. In this context, our group has developed a simple colorimetric method for detection of glucose by using peroxidase mimic material Fe-MIL-88NH_2 as a catalyst.[26] Later, we have reported Fe-MIL-88NH_2 can act as fluorescent probe and used for selective recognition of anti-cancer drug 6-mercaptopurine.[27] And as a dual colorimetric and fluorometric sensor, Fe-MIL-88NH_2 has also been designed for a wide rang of dopamine quantitative detection.[28] Moreover, we have found that the Fe-MIL-88NH_2 can be used for colorimetric determination of thiol compounds based on the competitive reaction between 3,3′,5,5′-tetramethylbenzidine (TMB) and thiol compounds with H_2O_2.[29] Although useful, the need for peroxidase substrate TMB added to the complexity of such detection strategies, and the colorimetric method was also limited by the sensitivity. Therefore, a new strategy is needed to overcome these problems. Similar to Fe-MIL-88NH_2, Fe-MIL-88 also exhibits highly peroxidase-like activity, and through combining with the AuNPs, we have applied Fe-MIL-88 for DNA hybridization detection.[30] Herein, we mainly studied catalytic activity of the Fe-MIL-88 and describe the use of Fe-MIL-88 for fluorescence sensing of biothiols.

Biological thiols such as cysteine (Cys), homocysteine (Hcy), and glutathione (GSH) play a crucial role in physiological processes[31, 32] and changes in the level of cellular thiols associate to diseases such as cancer and AIDS.[33, 34] Thus, a variety of analytical methods for monitoring these thiol compounds have been constructed.[35-40] Although these methods are promising, it is still necessary and significant for us to develop a simple as well as sensitive fluorescence platform for biothiols detection.

In this work, we have demonstrated a novel, simple strategy for sensitive determination of biothiols based on a "turn-on" fluorescence system made up of Fe-MIL-88 and H_2O_2. In the presence of hydrogen peroxide (H_2O_2), a weak fluorescence was observed in the supernatant of the Fe-MIL-88/H_2O_2 solution (Scheme 1). Upon adding biothiols such as GSH, Cys and Hcy to the Fe-MIL-88/H_2O_2 system, significant fluorescence enhancement could be observed. Moreover, the fluorescence enhancement was found to be proportional to the concentration of the biothiols added to the Fe-MIL-88/H_2O_2 solution, which permits biothiols to be quantitatively determined. Based on the phenomenon above, a novel fluorescence strategy for the determination of biothiols could be developed.

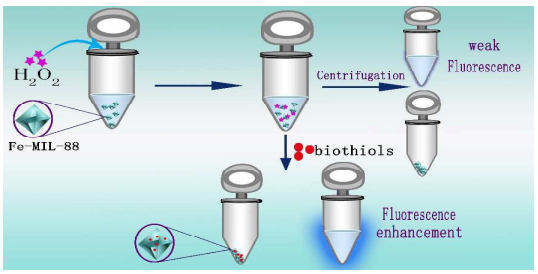

Scheme 1 Schematic illustration by using Fe-MIL-88 and H_2O_2 for the detection of biothiols.

2 Experimental

2.1 Apparatus

The fluorescence and the absorption spectra were recorded with a Hitachi F-2500 fluorescence spectrophotometer (Tokyo, Japan) and a Hitachi UV-3010 spectrophotometer (Tokyo, Japan), respectively. Fourier transform infrared (FTIR) spectra were recorded on a FITI-8400 (Shi-madzu, Japan) in the range of 4000-500 cm^{-1} using the KBr disk method. An S-4800 scanning electron microscope (SEM) (Hitachi, Japan) was used for imaging the size and shape of the Fe-MIL-88. Powder X-ray diffraction (PXRD) patterns were collected on an XD-3 X-ray diffractometer with Cu Kα radiation (λ = 1.5406 Å) in the range of 5-30θ at a scan rate of 2.0º min^{-1} (Purkinje, China).

2.2 Materials

Homocysteine (Hcy), cysteine (Cys), glutathione (GSH) and other amino acids were purchased from Beijing Dingguo Changsheng Biotech Co.,Ltd. $FeCl_3 \cdot 6H_2O$, H_2O_2 (30wt%), acetic acid, sodium acetate and thiourea were purchased from Chongqing Pharmaceutical Co., Ltd. Keyi Assay Glass Branch (Chongqing, China). Terephthalic acid (BDC) was purchased from Sigma-Aldrich (St. Louis, MO). Fe_3O_4 nanopowder (20 nm) was purchased from Aladdin Chemistry Co. Ltd. Serum samples were obtained from the Southwest University Hospital of Chongqing. All analytical reagents were used without further purification, and all solutions were prepared using ultra-pure water (18.2 MΩ).

2.3 Preparation of serum sample

For biothiols determination in serum, the serum samples of three healthy adults were first treated by spin dialysis at 12,000 rpm for 30 min, to ensure the concentration of biothiols in the linear range; the eluents were diluted ten times with doubly distilled water and directly used for experimental test.

2.4 General procedure

50 μL 0.2 M NaAc buffer solution (pH 5.4), 50 μL 0.6 mg mL^{-1} Fe-MIL-88 aqueous solution, and 30 μL of 5.0 mM H_2O_2 were added to a 1.5 mL EP vial. Afterwards, the appropriate amount of thiol compounds or serum solutions were added and the final mixture was diluted to 500 μL with ultra-pure water (18.2 MΩ). After mixing thoroughly, the solution was incubated at 40°C for 25 min, and in order to eliminate the interference from scattering background of Fe-MIL-88, centrifugation (16,000 rpm, 2 min) was thus conducted to remove the Fe-MIL-88 nanoparticles, and then the supernatant was transferred for fluorescence measurements using an F-2500 fluorescence spectrophotometer with an excitation wavelength of 326 nm, and the emission wavelength was recorded at 445 nm, PMT voltage (700 V).

3 Results and discussions

3.1 Spectral characteristic

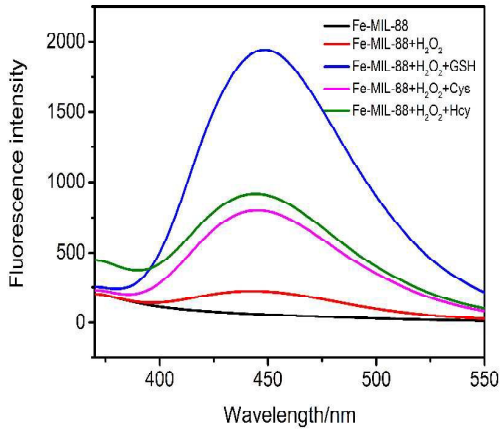

Fig. 1 The fluorescence emission spectra of Fe-MIL-88 (black), Fe-MIL-88+H_2O_2 (red), Fe-MIL-88+H_2O_2+GSH (blue), Fe-MIL-88+H_2O_2+Cys (pink), Fe-MIL-88+H_2O_2+Hcy (green). λ_{ex}, 326 nm; $c_{Fe\text{-}MIL\text{-}88}$, 0.06 mg mL^{-1}; c_{H2O2}, 0.3 mM; c_{GSH} = c_{Cys} = c_{Hcy} = 10μM; HAC-NaAC, pH 5.4; Time, 25 min; Temperature, 40°C.

As for Fe-MIL-88, we could not observe fluorescence in the wavelength range of 360~550 nm (Fig. 1), and only slight fluorescence signal could be seen upon addition of H_2O_2. The weak fluorescence most likely originated from the fluorescent hydroxylated terephthalic acid (OHBDC).[41] Since the Fe (III) on the surface of Fe-MIL-88 could catalyze the decomposition of H_2O_2 to produce •OH radicals through the Fenton-like reaction, which resulted in the partially conversion of the free ligand terephthalic acid (BDC) to strongly fluorescent hydroxylated terephthalic acid (OHBDC). Interestingly, on addition of biothiols such as GSH, Cys and Hcy to the Fe-MIL-88/H_2O_2 system, significant fluorescence enhancement could be observed. For comparison, the fluorescence of Fe-MIL-88/biothiols and H_2O_2/biothiols systems has also been investigated under the same conditions, as shown in Fig. S3A and B, unobservable fluorescence change means that the conjunct effects of Fe-MIL-88, H_2O_2 as well as biothiols are the main contributor to the fluorescence enhancement.

3.2 Optimum reaction conditions

To obtain the optimal condition for the determination of biothiols, the influences of experimental conditions including pH value, reaction time, Fe-MIL-88 concentration, as well as the H_2O_2 concentration were investigated initially with GSH. As shown in Fig. S4A, the fluorescence intensity of Fe-MIL-88/H_2O_2/GSH system conspicuously increases with pH value changed from 4.0 to 5.4. Meanwhile, the fluorescence intensity of Fe-MIL-88/H_2O_2 system exhibits negligible enhancement. According to the experimental results, the maximal enhanced fluorescence intensity was obtained at pH 5.4. And pH 5.4 of HAC-NaAC was thus chosen as the buffer system in further experiments. The effect of reaction time on the fluorescence enhancement is shown in Fig. S4B, the fluorescence enhancement of the Fe-MIL-88/H_2O_2 system caused by GSH almost completed within 25 min. Therefore, incubation time of 25 min was selected for subsequent

study. As illustrated in Fig. S4C, the fluorescence response of Fe-MIL-88/H_2O_2 towards GSH is strong as well as stable when the concentration of Fe-MIL-88 changed from 0.03 mg mL^{-1} to 0.09 mg mL^{-1}. To ensure the good reproducibility of the fluorescence system, 0.06 mg mL^{-1} was thus chosen as the optimum concentration of Fe-MIL-88. Additionally, the fluorescence value of Fe-MIL-88/H_2O_2/GSH system tended to increase with an increase in H_2O_2 concentration up to 0.3 mM while that of Fe-MIL-88/H_2O_2 changed little (Fig. S4D), and then H_2O_2 concentration of 0.3 mM was selected to offer strongest as well as stable fluorescence response. Although various biothiols at the same concentration had different fluorescence enhancement ability to the Fe-MIL-88/H_2O_2 system, the optimal condition for the detection of Cys and Hcy were same to that of GSH (Fig. S5 and Fig. S6).

3.3 Fluorescence enhancement mechanism

Compared with Fe-MIL-88/H_2O_2 system, no wavelength change was observed for Fe-MIL-88/H_2O_2/biothiols system (Fig. 1). In addition, the fluorescence emission of the Fe-MIL-88/H_2O_2/biothiols system all centered at 445 nm, we therefore presume that the enhanced fluorescence originated from hydroxylted terephthalic acid (OHBDC). Experiments were then carried out to confirm our speculation, with GSH as a modal biothiol. For the Fe-MIL-88/H_2O_2/GSH system, almost all the fluorescence products dispersed in the supernatant (Fig. 2A). Then we firstly investigated the UV-vis absorption spectrum of the supernatant, and Fig. 2B showed that the characteristic bands of the supernatant and the OHBDC were identical. The fluorescence spectrum of OHBDC has also been investigated based on CuS as catalyst since it could catalyze the conversion of weakly fluorescent BDC to strong fluorescent OHBDC in the presence of H_2O_2 (Fig. S7A).[42] As shown, the maximum emission of OHBDC centered at 443 nm, almost identical to that of the supernatant, all these observations reveals that the fluorescence product dispersed in the supernatant was the OHBDC. Moreover, both Fe-MIL-88 and iron (III) oxide (Fe_3O_4) have Fe-O clusters in there structure, but compared with Fe-MIL-88, no BDC consisted Fe_3O_4 nanopowder, and upon addition of H_2O_2 and GSH to the solution of Fe_3O_4 nanoparticals, no fluorescence change could be observed (Fig. S7B) further verified that the BDC is the main contributor in this fluorescence system.

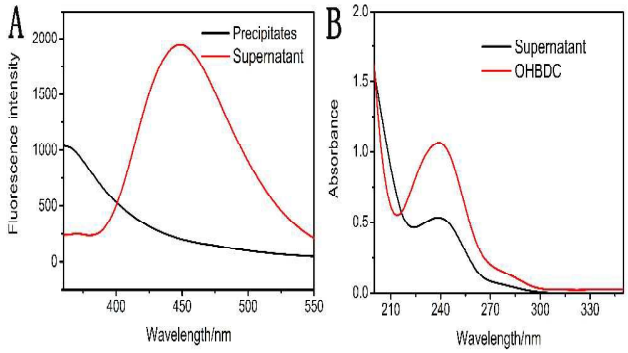

Fig. 2 (A) Fluorescence spectrum of supernatant (red) and precipitates (black) of the Fe-MIL-88/H_2O_2/GSH solution. (B) UV-vis absorption spectrum of the supernatant (black) and the OHBDC (red). $c_{Fe\text{-}MIL\text{-}88}$, 0.06 mg mL^{-1}, c_{H2O2}, 0.3 mM, c_{GSH}, 10 μM; HAC-NaAC, pH 5.4; λ_{ex}, 326 nm.

Since the fluorescence product has been proved to be OHBDC, it is necessary to investigate whether the Fe-MIL-88 is stable under the experimental conditions. After reaction, the morphology of the Fe-MIL-88 was examined by scanning electron microscopy (SEM) (Fig. 3A). As shown, no morphology change was observed for the Fe-MIL-88 after the reaction. Furthermore, the powder X-ray diffraction (XRD) pattern of the Fe-MIL-88 after the reaction is shown in Fig. 3B, the characteristic diffraction peaks remained and matched well with the as-prepared Fe-MIL-88, clearly indicating that the crystalline framework of Fe-MIL-88 was mostly maintained. These results demonstrate that the Fe-MIL-88 was stable under the experimental conditions employed here. And as we known, the channels of the as-synthesized Fe-MIL-88 are fully occupied by the unreacted ligand (BDC) and disordered organic solvents (DMF), if we dissolve the as-synthesized Fe-MIL-88 in water solution, some of the unreacted BDC within the channels could diffuse into the water via solvent exchange (DMF ↔ H_2O).[43] Therefore, we reasonably inferred that it is the unreacted as well as the occluded BDC contained in the Fe-MIL-88 that has been transformed to OHBDC in the presence of H_2O_2 and GSH.[44]

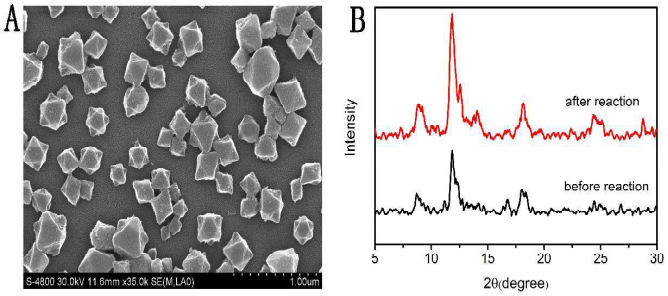

Fig. 3 (A) SEM images of Fe-MIL-88 after recation. (B) Powder XRD patterns of Fe-MIL-88 before (black) and after (red) reaction.

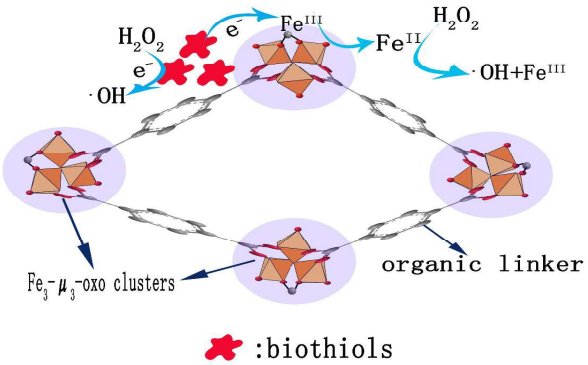

Fig. 4 Proposed mechanism for the biothiols detection by using Fe-MIL-88 and H_2O_2.

Based on the above observations, we speculate that the fluorescence enhancement mechanism is as follows (Fig. 4), on the one hand, biothiols could reduce H_2O_2 to produce •OH radicals directly.[45] On the other hand, the biothiols could adsorb on the surface of Fe-MIL-88, then biothiols could reduce the Fe^{3+} consisted in the Fe_3-μ_3-oxo clusters to generate Fe^{2+},[46] which is capable to activate H_2O_2 via the classic Fenton reaction to yield •OH radicals. Thus the resulted •OH radicals greatly enhanced

the conversion efficiency of the unreacted BDC within Fe-MIL-88 to fluorescent OHBDC, and then significant fluorescence turn-on was observed.

Firstly, studies were carried out to identify the presence of GSH on the surface of Fe-MIL-88. Fig. 5 shows the Energy dispersive X-ray spectroscopy (EDS) of Fe-MIL-88 before and after reaction. As shown, after reaction, the peak of S elements could be observed, which indicated that the presence of GSH on the surface of Fe-MIL-88. The FTIR spectroscopy has been recognized as an available tool to characterize the functional groups and the chemical interaction. As shown in Fig. 6A, the characteristic absorption peaks of the GSH at 2522 cm^{-1} was corresponding to the -SH vibration stretching, the band at 1712 cm^{-1} can be assigned to C=O asymmetrical stretching vibration, the 1600 and 1535 cm^{-1} bands were the deformation vibration of N-H in primary amine, and N-H in-plane bending vibration of secondary amine respectively. For free Fe-MIL-88, the 1562 cm^{-1} and 1411 cm^{-1} band could be assigned to benzene skeleton vibration. The broad peak centered at 3441 cm^{-1} was associated with the stretching vibrations of the O-H from the surface adsorbed water. As observed, the FTIR spectrum of the Fe-MIL-88 after reaction shows the stretching vibrations of the O-H at about 3414 cm^{-1}, which is red-shifted by 27 cm^{-1} with respect to that of the initial Fe-MIL-88 (3441 cm^{-1}). This red shift might be attributed to hydrogen-bonds between the Fe-MIL-88 and GSH. Moreover, after reaction, a new peak centered at 2952 cm^{-1} appeared in the spectrum of the Fe-MIL-88, which could mainly originate from the stretching vibration (υ (C-H)) in GSH (2950 cm^{-1}), further verified the presence of GSH in Fe-MIL-88. And the two peaks centered at 1650 and 1566 cm^{-1} could be assigned to C=O stretching vibration and benzene skeleton vibration of Fe-MIL-88, respectively.

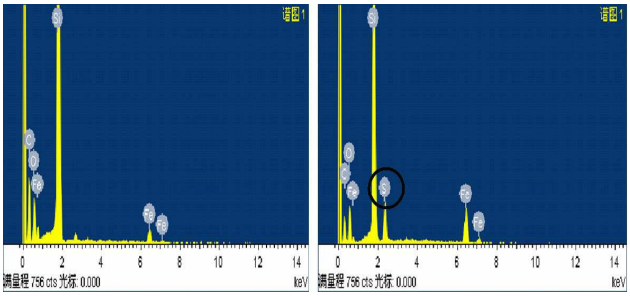

Fig. 5 Energy dispersive X-ray spectroscopy (EDS) of Fe-MIL-88 before (left) and after (right) reaction.

Besides, zeta potential measurement confirmed the existence of electrostatic interaction between Fe-MIL-88 and GSH. The Fe-MIL-88 is positive (Fig. 6B), while the GSH is negative under the detection condition. And after reaction, a significant decrease of the zeta-potential from +16.6 mV of free Fe-MIL-88 to -18.2 mV indicated the strong electrostatic interaction between Fe-MIL-88 and GSH. On the basis of the above discussion, it can be concluded that the GSH molecules could associate with Fe-MIL-88 via hydrogen bonding interaction as well as electrostatic interaction, thus provided the possibility of redox reaction between GSH and Fe^{3+} to generate Fe^{2+}, which is responsible for efficient decomposition of H_2O_2 to produce •OH radicals via the Fenton reaction.

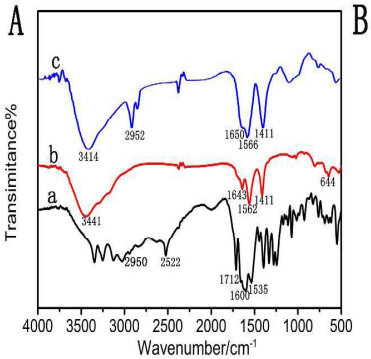

Sample name	Zeta-potential (mV)
GSH	-6.94
Fe-MIL-88,before reaction	+16.6
Fe-MIL-88,after reaction	-18.2

Fig. 6 (A) The FTIR spectroscopy of (a) GSH, (b) Fe-MIL-88 before reaction, and (c) Fe-MIL-88 after reaction. (B) Zeta-potential changes of Fe-MIL-88.

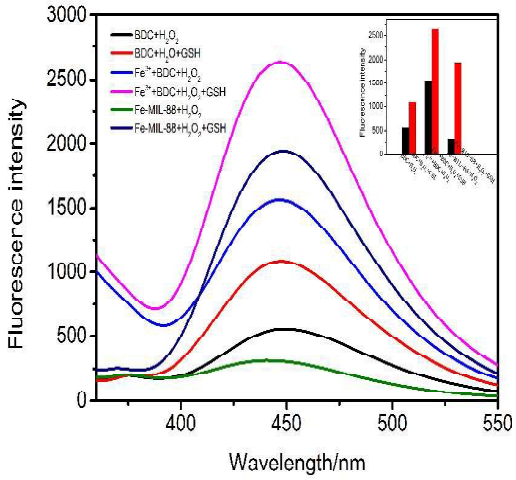

Fig. 7 The fluorescence emission spectra of the BDC+H_2O_2 (black), BDC+H_2O_2+GSH (red), Fe^{3+}+BDC+H_2O_2 (blue), Fe^{3+}+BDC+H_2O_2+GSH (pink), Fe-MIL-88+H_2O_2 (green), Fe-MIL-88+H_2O_2+GSH (dark blue). Inset histogram represents the fluorescence intensity of the above six systems. λ_{ex}, 326 nm; c_{Fe3+}, 0.06 mg mL^{-1}; c_{BDC},1mM; c_{H2O2}, 0.3 mM; c_{GSH},10μM. HAc-NaAc, pH 5.4.

Further experiments for validating the fluorescence enhancement mechanism were performed. As shown in Fig. 7, in the presence of GSH, fluorescence enhancement could be observed for BDC/H_2O_2 system, indicating that GSH could reduce H_2O_2 to produce •OH radicals. While upon addition of GSH to the Fe^{3+}/BDC/H_2O_2 system, the fluorescence enhancement became more obvious, which revealed the synergistic effects of GSH and the redox reaction between Fe^{3+} ions and GSH in the catalysis of BDC oxidation. Therefore, the proposed mechanism is further verified. On the other hand, both Fe-MIL-88 and Fe^{3+} exhibit catalytic activity toward oxidation of BDC in the presence of H_2O_2 and GSH, however, for the Fe-MIL-88/H_2O_2 system, the same concentrations of GSH would induce almost fivefold higher enhancement in the fluorescence intensity compared with that of the Fe^{3+}/BDC/H_2O_2 system (Fig. 7). Moreover, it should be noted that the nanomaterials that possess catalytic activity show great advantages such as ultrahigh stability, tunable catalytic activity, ease of separation, *etc.*[26, 30]

Considering the fact that redox reaction was likely to occur between the free Fe^{3+} ions in the Fe-MIL-88 solution and biothiols during which the electrons travel from the electron donor biothiols to the electron acceptor Fe^{3+} ions to generate Fe^{2+}.

It was necessary for us to eliminate the possibility that the enhanced fluorescence may be induced by the free iron ions leaching from the structure of Fe-MIL-88 in acidic solution. To test this, the same concentration of Fe-MIL-88 was first incubated in NaAc buffer (pH 5.4) for 30 min and then centrifuged at 16,000 rpm for 2 min to obtain the supernatant. Afterwards, H_2O_2 and BDC were added to the supernatant. Then catalytic activity of the supernatant was tested under optimal conditions. As shown in Fig. 8, upon addition of GSH to the supernatant/BDC/H_2O_2 system, fluorescence enhancement could be observed. However, the fluorescence change of the supernatant/BDC/H_2O_2 was relatively weak in comparison with that of Fe-MIL-88/H_2O_2 system. Moreover, as shown in Fig. 7, GSH could induce fluorescence enhancement of the BDC/H_2O_2 system, thus we propose that the effects between GSH and BDC/H_2O_2 play a major role in the fluorescence enhancement of the supernatant/BDC/H_2O_2 system. Based on the above discussion, we reasonably inferred that the high catalytic activity of Fe-MIL-88 toward oxidation of BDC was not originated from free iron ion, but indeed the metal center consisted in Fe-MIL-88 that played a dominant role in the catalysis of BDC oxidation.

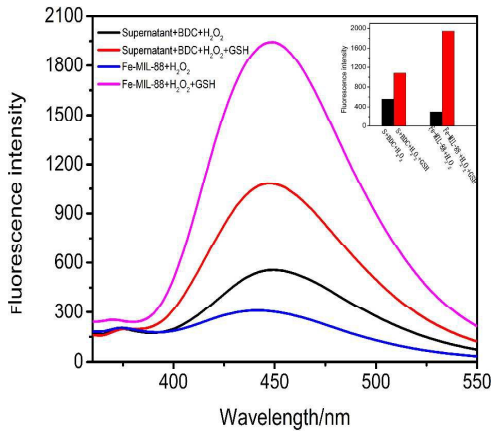

Fig. 8 The fluorescence emission spectra of the supernatant+BDC+H_2O_2 (black), supernatant+BDC+H_2O_2+GSH (red), Fe-MIL-88+H_2O_2 (blue), Fe-MIL-88+H_2O_2+GSH (pink). Inset histogram represents the fluorescence intensity of the above four systems. λ_{ex}, 326 nm; $c_{Fe\text{-}MIL\text{-}88}$, 0.06 mg mL^{-1}; c_{H2O2}, 0.3 mM; c_{BDC}, 1 mM; c_{GSH},10μM. HAc-NaAc, pH 5.4.

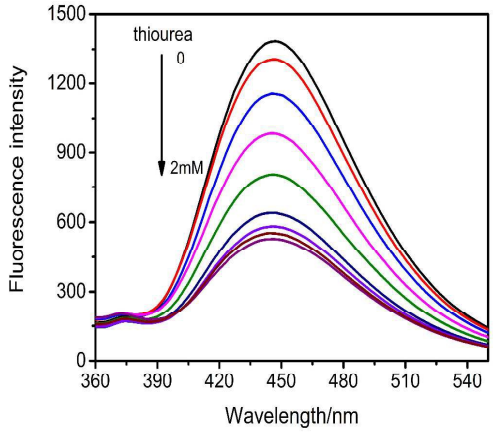

Fig. 9 The fluorescence spectra of Fe-MIL-88/H_2O_2/GSH system upon addition of thiourea.

Experiments were also performed to further insight into the crucial role that the •OH radicals played in this catalytic system. Since thiourea has been widely accepted as an effective radical scavenger of •OH,[47] it was therefore employed to detect •OH radicals (Fig. 9). As shown, when 0.7 mM thiourea was added to Fe-MIL-88/H_2O_2/GSH system, the fluorescence intensity of the system decreased by 60%, showing that •OH was indeed generated in the current solution and involved in a series of related reactions of this system, especially that it could react with BDC to produce highly fluorescent OHBDC. Moreover, the control experiment for Fe-MIL-88/H_2O_2 system upon addition of thiourea has also been carried out (Fig. S8). According to the result, the weak fluorescence of the Fe-MIL-88/H_2O_2 system could be quenched by thiourea, which further verified that the •OH radicals play a crucial role in the BDC oxidization.

3.4 Selectivity

Except for the requirement of sensitivity, good specificity was also needed, especially in real sample detection. To test the selectivity of the fluorescence enhancement behavior of biothiols, the effect of 18 other kinds of common biomolecules as well as some probable ions present in human blood serum were investigated and compared with that of biothiols. As shown in Fig. 10, the change of fluorescence intensities of Fe-MIL-88/H_2O_2 in the presence of Cys, Hcy, GSH were strikingly larger than that of other foreign substances. Therefore, the proposed method had high selectivity for biothiols and it was practical for the determination of biothiols in real samples.

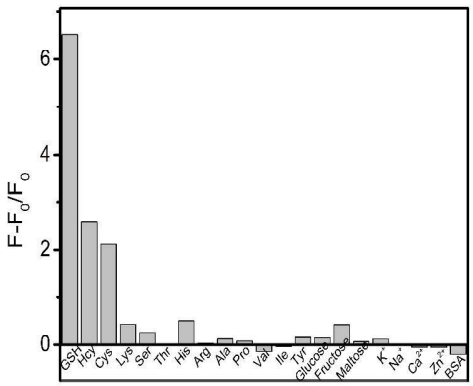

Fig. 10 Fluorescence response of the Fe-MIL-88/H_2O_2 system to various anions. F_0 and F are the fluorescence intensity of Fe-MIL-88/H_2O_2 system in the absence and presence of biothiols and the other analytes, respectively. Conditions: $c_{Fe\text{-}MIL\text{-}88}$, 0.06 mg mL^{-1}; c_{GSH} = c_{Cys} = c_{Hcy} = 10μM; c_{BSA}, 20 μg mL^{-1}; and others, 0.2 mM. Temperature, 40°C; Time, 25 min; HAc-NaAc, pH 5.4; λ_{ex}, 326 nm; λ_{em}, 445 nm.

3.5 Detection of biothiols in human serum

Using the optimized examining condition, the linearity of the method for detecting biothiols was calculated and expressed. Good linear relationships and low detection limits were obtained for GSH, Hcy and Cys (Fig. 11 and Table 1). To evaluate the applicability of the proposed method in real sample analysis, standard additions method was applied to detect the level of biothiols in human serum and the results were shown in Table 2.

The good recoveries (96~103%) of known amount GSH definitely demonstrated the accuracy and reliability of the present method for detecting biothiols in biological fluids.

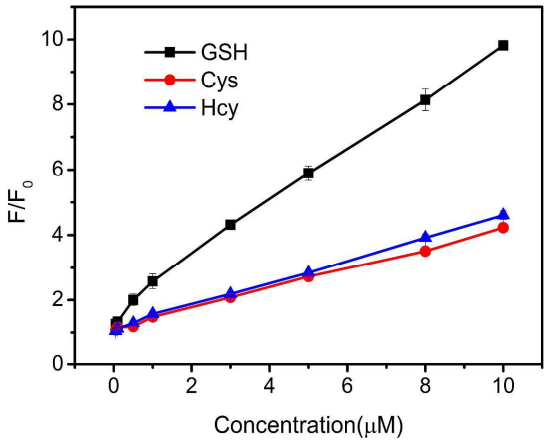

Fig. 11 Calibration plot for detection biothiols.

Table 1 Quantitative analyses of biothiols through the present method.

Analyte	Linear range(μM)	Regression equation	Correlation coefficient(R)	Detection limits(μM)
GSH	0.05-10.0	F/F_0=0.85c_{GSH}+1.44	0.994	0.03
Cys	0.05-10.0	F/F_0=0.33c_{Cys}+1.03	0.990	0.04
Hcy	0.05-10.0	F/F_0=0.36c_{Hcy}+1.11	0.992	0.04

Table 2 The determination of biothiols in three healthy human serums.

Sample	Amount found(μM)	Added (μM)	Found (μM)	Recovery (%)	R.S.D. (%)
Serum 1	4.04	0.5	4.52	96	2.6
Serum 2	3.01	1.0	4.0	99	2.3
Serum 3	4.02	2.0	6.08	103	6.0

4. Conclusion

In conclusion, upon adding biothiols to the Fe-MIL-88/H_2O_2 solution, significant fluorescence enhancement could be observed. Based on the phenomenon, a new assay for selective as well as sensitive recognition of biothiols has been established. The possible fluorescence enhancement mechanism has also been investigated, where it is revealed that the addition of biothiols to Fe-MIL-88/H_2O_2 system resulted in enhanced catalytic activity for H_2O_2 decomposition, which was due to the synergetic effect of biothiols as well as Fe^{3+} consisted in the Fe_3-μ_3-oxo clusters. On the one hand, biothiols could reduce H_2O_2 to produce •OH radicals. On the other hand, the biothiols could adsorb on the surface of Fe-MIL-88, then they can reduce the Fe^{3+} consisted in the Fe-MIL-88 to generate Fe^{2+}, which is capable to activate H_2O_2 via the classic Fenton reaction to produce •OH radicals. The above processes could cooperatively contribute to the activation of H_2O_2 to yield more amounts of •OH radicals, thus greatly enhanced the conversion efficiency of the unreacted BDC within Fe-MIL-88 to fluorescent OHBDC. Moreover, the spectrofluorometry method was successfully used for the detection of biothiols in human serum samples, which suggested the present approach had great practicability for diagnostic purposes.

ACKNOWLEDGEMENT

The authors are grateful for the financial support by the National Natural Science Foundation of China (NSFC, No. 21175109)

Notes and references

Key Laboratory of Luminescent and Real-Time Analytical Chemistry (Southwest University), Ministry of Education, College of Chemistry and Chemical Engineering, Southwest University, Chongqing 400715, China.

E-mail address: liyf@swu.edu.cn Tel.: (+86)23 68254659; Fax: (+86)23 68367257

† Electronic Supplementary Information (ESI) available: [details of any supplementary information available should be included here]. See DOI: 10.1039/b000000x/

1. S. T. Meek, J. A. Greathouse and M. D. Allendorf, *Adv. Mater.*, 2011, **23**, 249-267.
2. H. Furukawa, K. E. Cordova, M. O'Keeffe and O. M. Yaghi, *Science*, 2013, **341**, 1230444.
3. Z. Y. Gu, C. X. Yang, N. Chang and X. P. Yan, *Acc. Chem. Res.*, 2012, **45**, 734-745.
4. Z. Y. Gu and X. P. Yan, *Angew. Chem. Int. Ed.* , 2010, **49**, 1477-1480.
5. Z. Y. Gu, J. Q. Jiang and X. P. Yan, *Anal. Chem.*, 2011, **83**, 5093-5100.
6. N. Chang, Z. Y. Gu, H. F. Wang and X. P. Yan, *Anal Chem*, 2011, **83**, 7094-7101.
7. C. X. Yang, Y. J. Chen, H. F. Wang and X. P. Yan, *Chem. Eur. J.*, 2011, **17**, 11734-11737.
8. S. S. Liu, C. X. Yang, S. W. Wang and X. P. Yan, *Analyst*, 2012, **137**, 816-818.
9. Z. Y. Gu, Y. J. Chen, J. Q. Jiang and X. P. Yan, *Chem. Commun.*, 2011, **47**, 4787-4789.
10. S. H. Huo and X. P. Yan, *Analyst*, 2012, **137**, 3445-3451.
11. Y. Hu, Z. Huang, J. Liao and G. Li, *Anal. Chem.*, 2013, **85**, 6885-6893.
12. Y. Hu, H. Lian, L. Zhou and G. Li, *Anal. Chem.*, 2015, **87**, 406-412.
13. J. Liu, L. Chen, H. Cui, J. Zhang, L. Zhang and C. Y. Su, *Chem. Soc. Rev.*, 2014, **43**, 6011-6061.
14. D. Dang, P. Wu, C. He, Z. Xie and C. Duan, *J. Am. Chem. Soc.*, 2010, **132**, 14321–14323.
15. A. Dhakshinamoorthy, M. Alvaro and H. Garcia, *Chem. Commun.*, 2010, **46**, 6476-6478.
16. Z. Hu, B. J. Deibert and J. Li, *Chem. Soc. Rev.*, 2014, **43**, 5815-5840.
17. Y. Hu, J. Liao, D. Wang and G. Li, *Anal. Chem.*, 2014, **86**, 3955-3963.
18. C. X. Yang, H. B. Ren and X. P. Yan, *Anal. Chem.*, 2013, **85**, 7441-7446.
19. B. Chen, L. Wang, F. Zapata, G. Qian and E. B. Lobkovsky, *J. Am. Chem. Soc.*, 2008, **130**, 6718-6719.
20. B. Gole, A. K. Bar and P. S. Mukherjee, *Chem. Commun.*, 2011, **47**, 12137-12139.
21. Y. Liu, J. F. Eubank, A. J. Cairns, J. Eckert, V. C. Kravtsov, R. Luebke and M. Eddaoudi, *Angew. Chem. Int. Ed.*, 2007, **46**, 3278-3283.
22. J. R. Li, R. J. Kuppler and H. C. Zhou, *Chem. Soc. Rev.*, 2009, **38**, 1477-1504.
23. K. G. Laurier, F. Vermoortele, R. Ameloot, D. E. De Vos, J. Hofkens and M. B. Roeffaers, *J. Am. Chem. Soc.*, 2013, **135**, 14488-14491.
24. D. Wang, R. Huang, W. Liu, D. Sun and Z. Li, *ACS Catal.*, 2014, **4**, 4254-4260.
25. L. Shi , T. Wang , H. Zhang , K. Chang , X. Meng , H. Liu and J. Ye, *Adv. Sci.*, 2015, **2**, 1500006.
26. Y. L. Liu, X. J. Zhao, X. X. Yang and Y. F. Li, *Analyst*, 2013, **138**, 4526-4531.
27. Z. J. Sun, Y. L. Liu and Y. F. Li, *Spectrochim. Acta, Part A: Mol. Biomol. Spectrosc.*, 2015, **139**, 296-301.
28. C. Zhao, Y. L. Liu, X. L. Hu and Y. F. Li, *Anal. Sci.*, Accepted,
29. Z. W. Jiang, Y. L. Liu, X. L. Hu and Y. F. Li, *Anal. Methods*, 2014, **6**, 5647-5651.
30. Y. L. Liu, W. L. Fu, C. M. Li, C. Z. Huang and Y. F. Li, *Anal. Chim.*

Acta, 2015, **861**, 55-61.
31. Z. A. Wood, E. Schröder, J. R. Harris and L. B. Poole, *Trends Biochem. Sci.*, 2003, **28**, 32-40.
32. H. J. Forman, H. Zhang and A. Rinna, *Mol. Aspects. Med.*, 2009, **30**, 1-12.
33. S. C. Lu, *Mol. Aspects. Med.*, 2009, **30**, 42-59.
34. L. A. Herzenberg, S. C. De Rosa, J. G. Dubs, M. Roederer, M. T. Anderson, S. W. Ela, S. C. Deresinski and L. A. Herzenberg, *Proc. Natl. Acad. Sci.*, 1997, **94**, 1967-1972.
35. Y. Xiong, S. Chen, F. Ye, L. Su, C. Zhang, S. Shen and S. Zhao, *Chem. Commun.*, 2015, **51**, 4635-4638.
36. J. Wang and X. Qu, *Nanoscale*, 2013, **5**, 3589-3600.
37. Y. Zhang, Y. Li and X. P. Yan, *Anal. Chem.*, 2009, **81**, 5001-5007.
38. B. Han, J. Yuan and E. Wang, *Anal. Chem.*, 2009, **81**, 5569–5573.
39. R. R. Nawimanage, B. Prasai, S. U. Hettiarachchi and R. L. McCarley, *Anal. Chem*, 2014, **86**, 12266-12271.
40. Y. Tang, H. Song, Y. Su and Y. Lv, *Anal. Chem.*, 2013, **85**, 11876-11884.
41. L. Ai, C. Zhang, L. Li and J. Jiang, *Appl. Catal. B*, 2014, **148-149**, 191-200.
42. Q. W. Shu, J. Lan, M. X. Gao, J. Wang and C. Z. Huang, *CrystEngComm.*, 2015, **17**, 1374-1380.
43. A. P. Nelson, O. K. Farha, K. L. Mulfort and J. T. Hupp, *J. Am. Chem. Soc.*, 2009, **131**, 458-460.
44. M. H. Nguyen and Q. Nguyen, *J. Photoch. Photobio. A*, 2014, **288**, 55-59.
45. Y. Liu and F. Yu, *Nanotechnology*, 2011, **22**, 145704.
46. A. Amirbahman, L. Sigg and U. Gunten, *J. Colloid Interface Sci.*, 1997, **194**, 194-206
47. W. F. Wang, M. N. Schuchmann, H. P. Schuchmann, W. Knolle, J. V. Sonntag and C. V. Sonntag, *J. Am. Chem. Soc.*, 1999, **121**, 238-245.